Calculation on the Winding Factor and Armature Reaction MMF of a PMSM with 5-phase Fractional-slot Winding

Xuanfeng Shangguan
School of Electrical Engineering and Automatization, Henan Polytechnic University, Jiaozuo, China
Email: sgxf@hpu.edu.cn

Jiaolong Zhang and Wenli Zhang
School of Electrical Engineering and Automatization, Henan Polytechnic University, Jiaozuo, China
Email: zjl@hpu.edu.cn

***Abstract*—In this paper, a permanent magnet synchronous machine with fractional-slot and 5-phase winding is studied. By superposing of the back EMF (electro-motive force) phasors of all coil-sides in a phase winding, the winding factor of the machine is calculated. The idea of this calculation method is a clear, and operation is easy and fast. In normal working, one-phase open-circuit fault, open-circuit fault of two adjacent phases, and open-circuit fault of two non adjacent phases states, the armature MMFs (electro-motive forces) are calculated, and the contents of their harmonics are analyzed, the forward and reverse rotating MMFs are discussed. The drawn results can be applied to analyze the running states of the machines, guide machine design and control.**

***Index Terms*—winding factor, magnetic-motive force, fractional-slot, 5-phase winding, fault state**

I. INTRODUCTION

Fractional-slot PMSMs (permanent magnet synchronous machines) have been gaining wide interest over the past decade [1-5]. The literature [1] has done a very good job in summarizing the features, recent researches and developments, applications, challenges of fractional-slot PMSMs. The machines own the some advantages such as high-power density, high efficiency, low cogging torque, short end winding, low copper loss, high flux-weakening capability. At present，the research works mainly concentrate on the combination of slot and pole number, torque ripple reduction, rotor loss [2], unbalanced magnetic pull, space harmonic analysis of the MMFs, optimization design, etc. Fractional-slot PMSMs may have many poles and low speed, so, are suitable for direct drive systems, such as electric bikes, hybrid vehicle, hoists, etc.

Multiphase motor drives possess many advantages over the traditional 3-phase motor drives [6-10], these include fault tolerant and reducing the amplitude of torque pulsation, reducing the stator current per phase without increasing the voltage per phase. So, Multiphase motor drives are in applications where high reliability is demanded such as electric/hybrid vehicles, aerospace applications, ship propulsion and high power applications. The research works mainly concentrate on machine optimization design and performance control in the fault states.

This paper will discuss a fractional-slot PMSM with 4 poles, 15 slots, and 5-phase double-layer winding. The surface-mounted permanent magnet poles are radially magnetized. Firstly, this paper drew the star of slots of the prototype, on the basis, obtained the three layouts of 5-phase windings, the coils are 4-solt span, 3-solt span, and 2-solt span respectively, and calculated the winding factors of the different coil spans. Then, in the normal work condition, the MMFs of per phase winding and the resultant MMF of 5-phase windings were calculated, and the harmonic contents of the resultant MMF were analyzed. Thirdly, in the cases of one-phase open-circuit fault, open-circuit fault of two adjacent phases, and open-circuit fault of two non adjacent phases states, the armature resultant MMFs were analyzed, the rotating MMFs were discussed.

II. STAR OF SLOTS AND WINDING LAYOUT

In order to draw the slot star of the analyzed prototype, first of all, according to the given specification, the electrical angle between adjacent two stator slots is obtained

$$\alpha = \frac{p \cdot 360°}{Q} = \frac{720°}{15} = 48°$$

Where, p is the number of pole pairs, Q is the number of the stator slots.

Then, the EMF phasors of coil side in per stator slot can be shown as Fig.1.

The slot number of per pole per phase (SNPP)

$$q = \frac{Q}{2pm} = \frac{15}{2 \times 2 \times 5} = 0.75$$

SNPP is a fractional number less than one, so, the winding is fractional slot winding.

According to the law to get the maximum resultant EMFs, the coil sides in 15 stator slots are assigned to five

doi:10.4304/jcp.8.3.725-732

phases. Each phase winding includes six coil sides, they can form 3 coils.

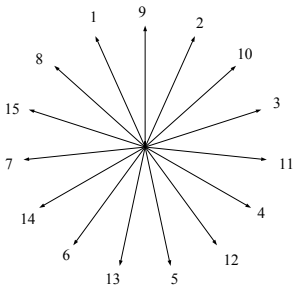

Figure.1 Star of slots

The three kinds of coil spans adopted are respectively 4, 3, and 2 slot-pitchs. By the star of slots, winding layouts are determined in Fig.2.

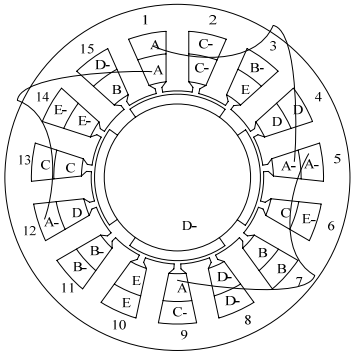

(a) Coil span = 4

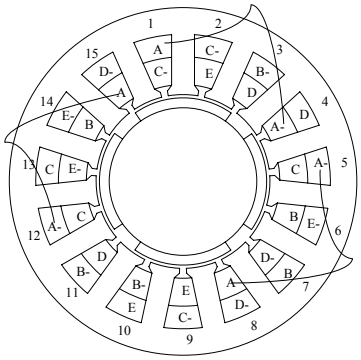

(b) Coil span = 3

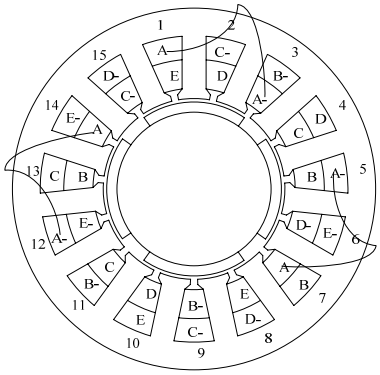

(c) Coil span = 2

Figure.2 Winding layouts of 5-phase PMSMs with 15 stator slots

III. CALCULATION OF WINDING FACTOR

Winding factor depends on three sub factors (pitch factor, distribution factor and skewing factor). Each of the sub factors can be easily calculated for conventional integer slot distributed windings with well-known formulas. However, these factors are hard to visualize in fractional-slot windings. In this paper, the method to calculate winding factor by the back EMF of each coil-side from the star of slots has some advantages such as ideas are clear, calculation easy.

A. Winding Factor Calculation of 4-Solt Span Coil

According to the each coil layout of A-phase winding shown in Fig.2(a), the upper coil side in slot-1 and the lower coil side in slot-5 form the first coil of A-phase winding, the upper coil side in slot-5 and the lower coil side in slot-9 form the second coil, the upper coil side in slot-12 and the lower coil side in slot-1 form the third coil. It is shown the phase angle difference between the two sides of each coil is 192° electrical degree ($4\alpha=4\times48^{o}=192^{o}$). The three coils of each phase winding are in series. The back EMF phasors of six coil sides of A- phase winding are shown in Fig.3(a). The back EMF of the first coil is the resultant of $\dot{E}_{1A+}$ and $\dot{E}_{5A-}$. The back EMF of the second coil is the resultant of $\dot{E}_{5A-}$ and $\dot{E}_{9A+}$. The back EMF of the third coil is the resultant of $\dot{E}_{12A-}$ and $\dot{E}_{1A+}$. The phase angle differences of the back EMF of the coils are 12° electrical degree, not in the same phase. So, it isn't feasible that the three coils are in parallel.

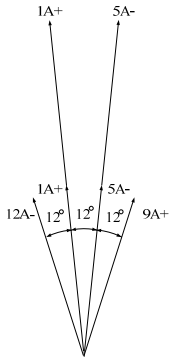

(a) Coil span = 4

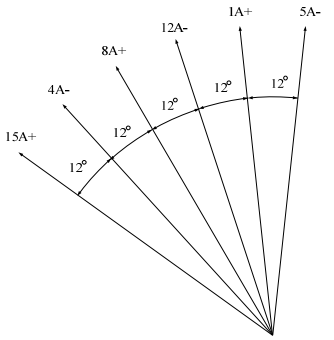

(b) Coil span = 3

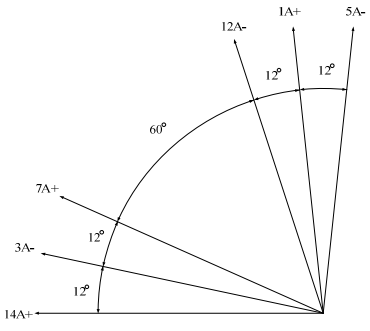

(c) Coil span = 2

Figure.3 Back EMF phasors of the coil sides in A-phase winding

The back EMF phasor of *i*-th coil side is expressed with $\dot{E}_i$. According to phasor diagram Fig.3(a), the relutant EMF and the winding factor of A-phase winding can be calculated (the three coils of each phase winding in series).

$$k_{w1} = \frac{\left|\sum_{i=1}^{6} \dot{E}_i\right|}{6E} = \frac{\left(\sqrt{2\times 2^2 + 2\times 2^2 \times \cos 12°} + \sqrt{2\times 1^2 + 2\times 1^2 \times \cos 36°}\right)E}{6E} = 0.98$$

B. Winding Factor Calculation of 3-Solt Span Coil

According to Fig. 2 (b), the upper coil side in slot-1 and the lower coil side in slot-4 form the first coil of A-phase winding. The upper coil side in slot-5 and the lower coil side in slot-8 form the second coil. The upper coil side in slot-12 and the lower coil side in slot-15 form the third coil. It is shown the phase angle difference between the two sides of each coil is 144 ° electrical degree (3α=3×48º=144º). The back EMF phasors of the six coil sides in A-phase winding is shown in Fig. 3(b). The back EMF of the first coil is the resultant of $\dot{E}_{1A+}$ and $\dot{E}_{4A-}$. The back EMF of the second coil is the resultant of $\dot{E}_{5A-}$ and $\dot{E}_{8A+}$. The back EMF of the third coil is the resultant of $\dot{E}_{12A-}$ and $\dot{E}_{15A+}$. In Fig.3 (b), the phase angle differences of the back EMF of the coils are 12° electrical degree.

Winding factor of A-phase winding can be obtained.

$$k_{w1} = \frac{\sum_{i}^{6} \dot{E}_i}{6E} = \frac{1}{6E}\left(\sqrt{2\times 1^2 + 2\times 1^2 \cos 12°} + \sqrt{2\times 1^2 + 2\times 1^2 \cos 36°} + \sqrt{2\times 1^2 + 2\times 1^2 \cos 60°}\right)E = 0.9371$$

C. Winding Factor Calculation of 2-Solt Span Coil

According to Fig. 2 (c), the upper coil side in slot-1 and the lower coil side in slot-3 form the first coil. The upper coil side in slot-5 and the lower coil side in slot-7 form the second coil. The upper coil side in slot-12 and the lower coil side in slot-14 form the third coil. It is shown the phase angle difference between the two sides of each coil is 96° electrical degree (2α=2×48º=96º). The back EMF phasors of the coil sides of A-phase winding are shown in Fig.3(c). The back EMF of the first coil is the resultant of $\dot{E}_{1A+}$ and $\dot{E}_{3A-}$. The back EMF of the second coil is the resultant of $\dot{E}_{5A-}$ and $\dot{E}_{7A+}$. The back EMF of the third coil is the resultant of $\dot{E}_{12A-}$ and $\dot{E}_{14A+}$. In Fig.3(c), the phase angle differences of the back EMF of the coils are 12° electrical degree.

Winding factor of A-phase winding can be obtained.

$$k_{w1} = \frac{\sum_{i}^{6} \dot{E}_i}{6E} = \frac{1}{6E}\left(\sqrt{2\times 1^2 + 2\times 1^2 \cos 60°} + \sqrt{2\times 1^2 + 2\times 1^2 \cos 84°} + \sqrt{2\times 1^2 + 2\times 1^2 \cos 108°}\right)E = 0.732$$

The highest winding factor can be obtained with 4-solt span coil (the coil span is closest to pole pitch, 3.75 times the slot pitch), the lowest with 2-solt span coil.

IV. MMF OF ARMATURE

A. Armature Currents and MMF of 5-Phase Machine

The armature currents of 5-phase machine can be expressed with formula (1).

$$\begin{cases} i_A = I_m \sin(\omega t) \\ i_B = I_m \sin(\omega t - 2\pi/5) \\ i_C = I_m \sin(\omega t - 4\pi/5) \\ i_D = I_m \sin(\omega t - 6\pi/5) \\ i_E = I_m \sin(\omega t - 8\pi/5) \end{cases} \quad (1)$$

The armature MMF of a 5-phase machine is the resultant MMF of the 5 phase windings. The MMF is a function of time variable *t* and space variable *θ*.

$$f(\theta,i) = f_A(\theta,i_A) + f_B(\theta,i_B) + f_C(\theta,i_C) + f_D(\theta,i_D) + f_E(\theta,i_E) \quad (2)$$

The MMF of M-phase winding (M is A, B, C, D, and E) can be expressed with formula (3).

$$f_M(\theta,i_M) = \sum_{i=1}^{n} f_{Mi}(\theta,i_M) \quad (3)$$

where, $f_{Mi}(\theta,i_M)$ is the MMF of *i*th-coil in M-phase winding, *n* is the number of the coils in per phase winding.

$$f_{Mi}(\theta,i_M) = \begin{cases} \dfrac{(Q-S)}{Q} i_M N_c & \theta \in (\theta_{i1} \sim \theta_{i2}) \\ \dfrac{S}{Q} i_M N_c & other \end{cases} \quad (4)$$

where, N_c is the turn number of per coil, *S* is coil span in number of slots, i_M is the current of M-phase winding. Angle θ_{i1} and θ_{i2} express positions of the two sides of *i*th-coil.

B. MMF of a Phase Winding

At $\omega t = \pi/2$, A-phase current reaches the biggest value. $i_A = I_m$, $i_B = 0.309 I_m$, $i_C = -0.809 I_m$, $i_D = -0.809 I_m$, $i_E = 0.309 I_m$.

When the 4-solt span coils are used, the MMFs of the three coils in A-phase winding are expressed respectively in Fig.4(a) ~ (c). The resultant MMF of the three coils is expressed in Fig.4 (d).

By similar way, the MMFs of the other four phase windings can be obtained.

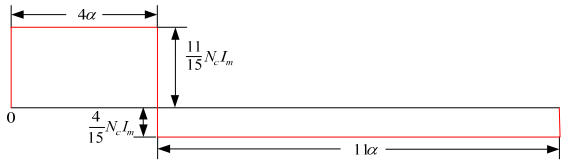

(a) Coil-1

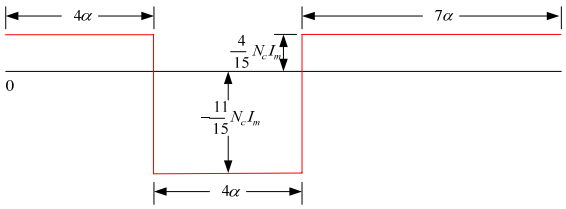

(b) Coil-2

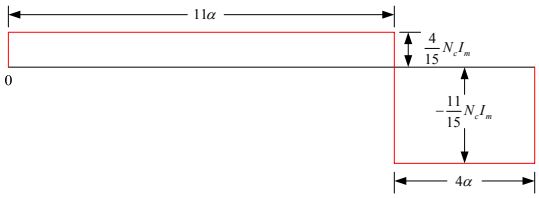

(c) Coil-3

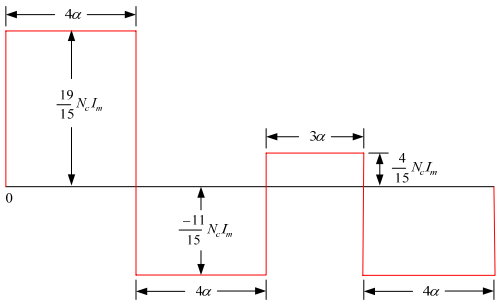

(d) Resultant MMF

Figure.4 MMF of A-phase winding

C. Resultant Armature MMF of the 5 Phase Windings

Fig.5 (a) and (b) show respectively the resultant armature MMF and its harmonics. Per unit of vertical axis expresses $N_cI_m/15$ ampere-turns, the followings are the same.

The first order harmonic varies one period along the air-gap circumference, and the main harmonic has two periods (4-pole machine). The main harmonic is the component to develop effective electro-magnetic torque. But the main harmonic, there are other influential harmonics, such as thirteenth harmonic, seventeen harmonic, and twenty-eighth harmonic. Fig.5 shows the amplitude of the first order harmonic is very small.

The main harmonic of the MMF develops a round rotating magnetic field.

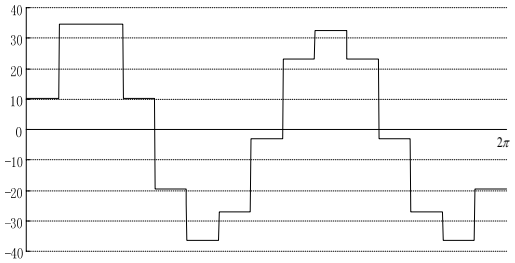

(a) Armature MMF

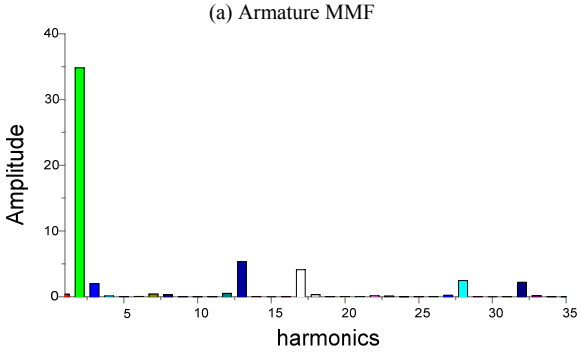

(b) Harmonic contents

Figure.5 Resultant MMF and its harmonic contents of 5- phase winding

D. Armature MMF at One-Phase Winding Open-Circuit Fault

In this section, let us suppose that the A-phase winding is permanently open, i.e., i_A =0. The MMFs of 5 phase windings are expressed with formula (5).

$$\begin{cases} f_{A1}=0 \\ f_{B1}=F_{m1}\cos(\theta-2\pi/5)\cos(\omega t-2\pi/5) \\ \quad=\frac{1}{2}F_{m1}\cos(\theta+\omega t-2\times2\pi/5)+\frac{1}{2}F_{m1}\cos(\theta-\omega t) \\ \quad=f_{B1}^{-}+f_{B1}^{+} \\ f_{C1}=F_{m1}\cos(\theta-2\times2\pi/5)\cos(\omega t-2\times2\pi/5) \\ \quad=\frac{1}{2}F_{m1}\cos(\theta+\omega t-4\times2\pi/5)+\frac{1}{2}F_{m1}\cos(\theta-\omega t) \\ \quad=f_{C1}^{-}+f_{C1}^{+} \\ f_{D1}=F_{m1}\cos(\theta-3\times2\pi/5)\cos(\omega t-3\times2\pi/5) \\ \quad=\frac{1}{2}F_{m1}\cos(\theta+\omega t-6\times2\pi/5)+\frac{1}{2}F_{m1}\cos(\theta-\omega t) \\ \quad=f_{D1}^{-}+f_{D1}^{+} \\ f_{E1}=F_{m1}\cos(\theta-4\times2\pi/5)\cos(\omega t-4\times2\pi/5) \\ \quad=\frac{1}{2}F_{m1}\cos(\theta+\omega t-8\times2\pi/5)+\frac{1}{2}F_{m1}\cos(\theta-\omega t) \\ \quad=f_{E1}^{-}+f_{E1}^{+} \end{cases} \tag{5}$$

The resultant MMF is calculated.

$$f_1=f_{B1}+f_{C1}+f_{D1}+f_{E1} \tag{6}$$

Since the MMFs of 5 phase windings are asymmetric, the main harmonic of the resultant MMF develops an elliptic rotating magnetic field. The elliptic rotating magnetic field can be decomposed into the forward rotating magnetic field and reverse rotating magnetic field.

The forward round rotating MMF is calculated.

$$f_1^{+}=f_{B1}^{+}+f_{C1}^{+}+f_{D1}^{+}+f_{E1}^{+}=2F_{m1}\cos(\theta-\omega t) \tag{7}$$

The reverse round rotating MMF is calculated.

$$
\begin{aligned}
f_1^- &= f_{B1}^- + f_{C1}^- + f_{D1}^- + f_{E1}^- \\
&= \frac{1}{2}F_{m1}\left[\cos\left(\theta+\omega t-2\times\frac{2\pi}{5}\right)+\cos\left(\theta+\omega t-4\times\frac{2\pi}{5}\right)\right. \\
&\quad \left.+\cos\left(\theta+\omega t-6\times\frac{2\pi}{5}\right)+\cos\left(\theta+\omega t-8\times\frac{2\pi}{5}\right)\right] \\
&= \frac{1}{2}F_{m1}\cdot 4\cos(\theta+\omega t)\cos\frac{4\pi}{5}\cos\frac{2\pi}{5} \\
&= -2\times\frac{\sqrt{5}-1}{4}\times\frac{\sqrt{5}+1}{4}\times F_{m1}\cos(\theta+\omega t) \\
&= -\frac{1}{2}F_{m1}\cos(\theta+\omega t)
\end{aligned}
\tag{8}
$$

At $\omega t=\pi/2$, the resultant MMF of 5 phase windings is expressed in Fig.6 (a).

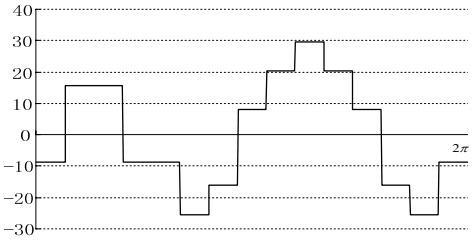

(a) Armature MMF

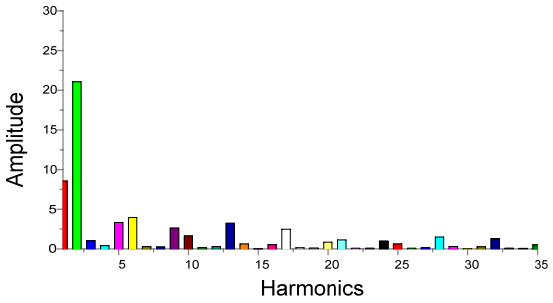

(b) Harmonic content

Figure.6 Armature MMF and its harmonic contents at A-phase open-circuit fault

Fig.6 (b) shows that the amplitude of the main harmonic decreases from 34.8 to 21.05 and the amplitude of the first order harmonic increases significantly.

E. Improvement of the Armature MMF at One-Phase Open-Circuit Fault

According to literature [7], each healthy phase maintains the same current amplitude, and the current phases of the B-phase and the E-phase are regulated, as shown in Fig.7. $\beta=\pi/5, \delta=\gamma=0, \varepsilon=-\pi/5$.

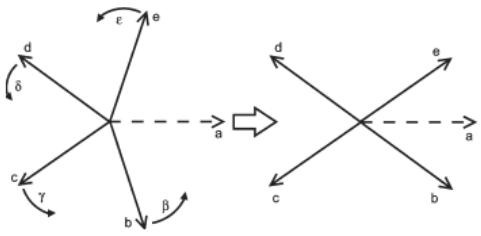

Figure.7. Current phasor diagram of open-circuit fault of A-phase

Then, the resultant MMFs of 5 phase windings are given in formula (9).

$$
\begin{cases}
f_{A1}=0 \\
f_{B1}=F_{m1}\cos(\theta-2\pi/5)\cos(\omega t-2\pi/5+\pi/5) \\
\quad =\frac{1}{2}F_{m1}\cos\left(\theta-\omega t-\frac{\pi}{5}\right)+\frac{1}{2}F_{m1}\cos\left(\theta+\omega t-\frac{3\pi}{5}\right) \\
\quad =f_{B1}^+ + f_{B1}^- \\
f_{C1}=F_{m1}\cos(\theta-2\times 2\pi/5)\cos(\omega t-2\times 2\pi/5) \\
\quad =\frac{1}{2}F_{m1}\cos(\theta-\omega t)+\frac{1}{2}F_{m1}\cos\left(\theta+\omega t-\frac{8\pi}{5}\right) \\
\quad =f_{C1}^+ + f_{C1}^- \\
f_{D1}=F_{m1}\cos(\theta-3\times 2\pi/5)\cos(\omega t-3\times 2\pi/5) \\
\quad =\frac{1}{2}F_{m1}\cos(\theta-\omega t)+\frac{1}{2}F_{m1}\cos\left(\theta+\omega t-\frac{12\pi}{5}\right) \\
\quad =f_{D1}^+ + f_{D1}^- \\
f_{E1}=F_{m1}\cos(\theta-4\times 2\pi/5)\cos(\omega t-4\times 2\pi/5-\pi/5) \\
\quad =\frac{1}{2}F_{m1}\cos\left(\theta-\omega t+\frac{\pi}{5}\right)+\frac{1}{2}F_{m1}\cos\left(\theta+\omega t-\frac{17\pi}{5}\right) \\
\quad =f_{E1}^+ + f_{E1}^-
\end{cases}
\tag{9}
$$

The forward round rotating MMF is calculated.

$$
\begin{aligned}
f_1^+ &= f_{B1}^+ + f_{C1}^+ + f_{D1}^+ + f_{E1}^+ \\
&= F_{m1}\cos(\theta-\omega t)\left(1+\cos\frac{\pi}{5}\right) \\
&= \frac{5+\sqrt{5}}{4}F_{m1}\cos(\theta-\omega t)
\end{aligned}
\tag{10}
$$

The reverse round rotating MMF is calculated.

$$
f_1^- = f_{B1}^- + f_{C1}^- + f_{D1}^- + f_{E1}^- = 0 \tag{11}
$$

So, the main harmonic of the MMF develops a forward round rotating MMF only.

At $\omega t=\pi/2$, the resultant armature MMF of the other 4 phase windings is expressed in Fig. 8.

Fig.8 (b) shows the amplitude of main harmonic increases to 25.392 from 21.05, the improved result is visible. The amplitude of the first order harmonic increases significantly.

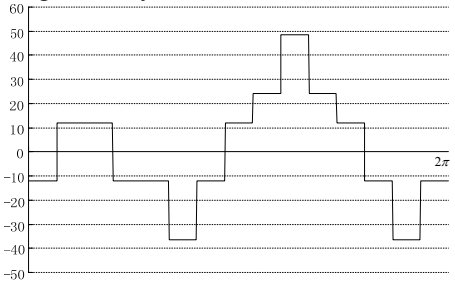

(a) Resultant MMF

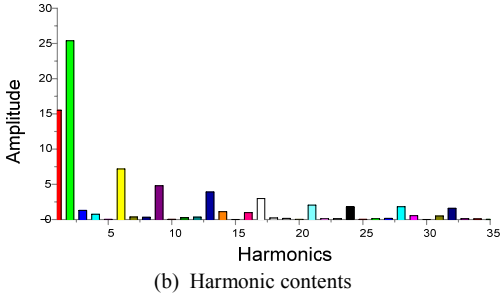

(b) Harmonic contents

Figure.8. Armature MMF and its harmonic contents after improvement

F. Armature MMF at Two-Phase Winding Open-Circuit Fault

1) open-circuit fault of two adjacent phases

In this section, let us suppose that the A-phase and B-phase windings are permanently open, i.e., $i_A = i_B = 0$.

The resultant MMF of other three phase windings is calculated.

$$f_1 = f_{C1} + f_{D1} + f_{E1} \tag{12}$$

The forward round rotating MMF is calculated.

$$\begin{aligned} f_1^+ &= f_{B1}^+ + f_{D1}^+ + f_{E1}^+ \\ &= \frac{3}{2} F_{m1} \cos(\theta - \omega t) \end{aligned} \tag{13}$$

The reverse round rotating MMF is calculated.

$$\begin{aligned} & f_1^- = f_{C1}^- + f_{D1}^- + f_{E1}^- \\ &= \frac{1}{2} F_{m1} \left[\cos\left(\theta + \omega t - \frac{4\pi}{5}\right) + \cos\left(\theta + \omega t - \frac{6\pi}{5}\right) + \cos\left(\theta + \omega t - \frac{8\pi}{5}\right) \right] \\ &= \frac{1}{2} F_{m1} \cdot \cos\left[(\theta + \omega t) - 6 \times \frac{2\pi}{5} \right] \left[2\cos\left(2 \times \frac{2\pi}{5}\right) + 1 \right] \\ &= \frac{3 - \sqrt{5}}{4} F_{m1} \cdot \cos\left((\theta + \omega t) - \frac{2\pi}{5} \right) \end{aligned} \tag{14}$$

At $\omega t = \pi / 2$, the resultant armature MMF of C-phase, D-phase, and E-phase windings is expressed in Fig. 9(a).

Fig.9 (b) shows the amplitude of main harmonic is 20.15, the amplitude of the first order harmonic is 6.62.

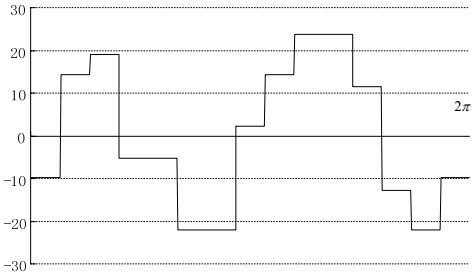

(a) Resultant MMF

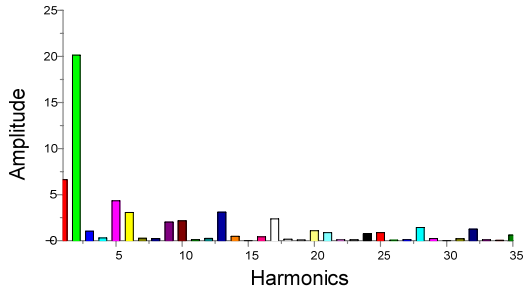

(b) Harmonic content

Figure.9 Armature MMF and its harmonic contents (open-circuit fault of A and B-phase windings)

2) open-circuit fault of two nonadjacent phases.

In this section, let us suppose that the A-phase and C-phase windings are permanently open, i.e., $i_A = i_C = 0$.

The resultant MMF of other three phase windings is calculated.

$$f_1 = f_{B1} + f_{D1} + f_{E1} \tag{15}$$

The forward round rotating MMF is calculated.

$$\begin{aligned} f_1^+ &= f_{B1}^+ + f_{D1}^+ + f_{E1}^+ \\ &= \frac{3}{2} F_{m1} \cos(\theta - \omega t) \end{aligned} \tag{16}$$

The reverse round rotating MMF is calculated.

$$\begin{aligned} & f_1^- = f_{B1}^- + f_{D1}^- + f_{E1}^- \\ &= \frac{1}{2} F_{m1} \left[\cos\left(\theta + \omega t - \frac{2\pi}{5}\right) + \cos\left(\theta + \omega t - \frac{6\pi}{5}\right) + \cos\left(\theta + \omega t - \frac{8\pi}{5}\right) \right] \\ &= \frac{1}{2} F_{m1} \left\{ \frac{\sqrt{5} - 1}{2} \left[\cos(\theta + \omega t)\cos\frac{\pi}{5} - \sin(\theta + \omega t)\sin\frac{\pi}{5} \right] \right. \\ &\quad \left. - \cos(\theta + \omega t)\cos\frac{\pi}{5} - \sin(\theta + \omega t)\sin\frac{\pi}{5} \right\} \\ &= \frac{1}{2} F_{m1} \left[\frac{1 - \sqrt{5}}{4} \cos(\theta + \omega t) - \frac{1}{4}\sqrt{10 + 2\sqrt{5}} \sin(\theta + \omega t) \right] \\ &= \frac{1}{2} F_{m1} \cdot K_m \cos[(\theta + \omega t) - \phi] \end{aligned} \tag{17}$$

where

$$K_m = \left[\left(\frac{1 - \sqrt{5}}{4} \right)^2 + \left(\frac{\sqrt{10 + 2\sqrt{5}}}{4} \right)^2 \right]^{\frac{1}{2}} = 1 \tag{18}$$

$$\phi = \tan^{-1}\left[\frac{-\frac{1}{8}\left(1 + \sqrt{5}\right)\sqrt{10 - 2\sqrt{5}}}{\frac{1 - \sqrt{5}}{4}} \right] = \tan^{-1}\left(\frac{5 + \sqrt{5}}{3 - \sqrt{5}} \right)^{\frac{1}{2}} \tag{19}$$

At $\omega t = \pi / 2$, the resultant armature MMF of B-phase, D-phase, and E-phase windings is expressed in Fig. 10 (a).

Fig.10 (b) shows the amplitude of main harmonic is 13.62, the amplitude of the first order harmonic is 9.22.

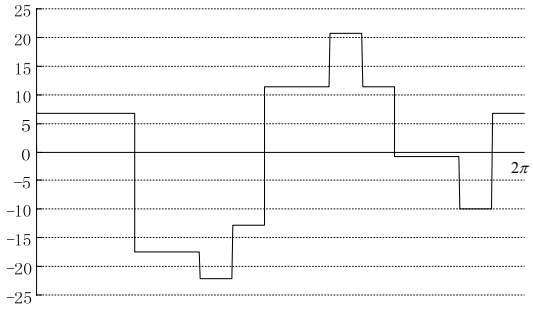

(a) Resultant MMF

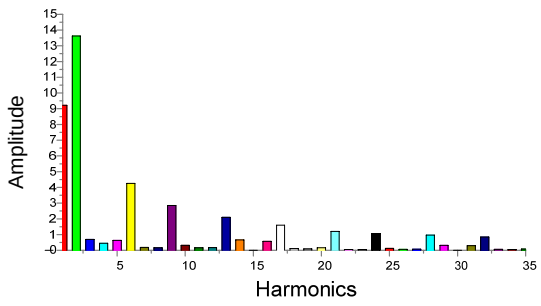

(b) Harmonic content

Figure.10 Armature MMF and its harmonic contents (open-circuit fault of A and C-phase windings)

By analysis and comparison, open-circuit fault of two non adjacent phase windings is more serious, the main

harmonic is smaller, the operation state of the motor is worse.

V. Flux Density Distribution Of The Armature Reaction Magnetic Field

In Fig.11, Fig.12, and Fig.13, with different coil spans, the air gap flux density distributions of the armature reaction fields and their harmonic contents are shown, without permanent magnets.

When the coils are 4-solt span, the amplitude of main harmonic is the largest. The coils are 2-solt span, and the amplitude of main harmonic is the smallest. The amplitude of the main harmonic of 3-solt span coils is close to that of 4-solt span coils. When the coils are 3-solt span, the end windings are short and material and energy loss can be reduced, so, should be given priority in the application.

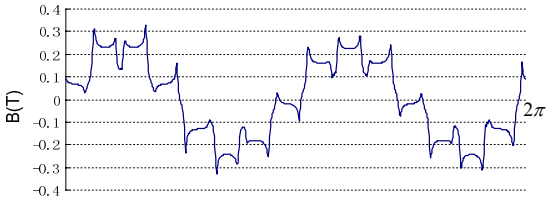

(a) Flux density distribution

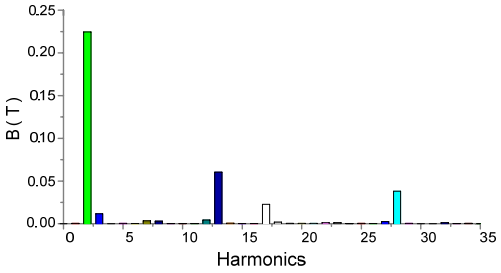

(b) Harmonic contents

Figure.11 Flux density and its harmonic contents (coil span = 4)

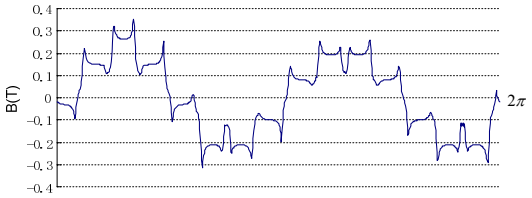

(a) Flux density distribution

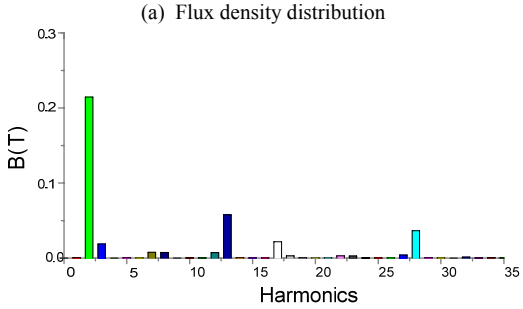

(b) Harmonic contents

Figure.12 Flux density and its harmonic contents (coil span = 3)

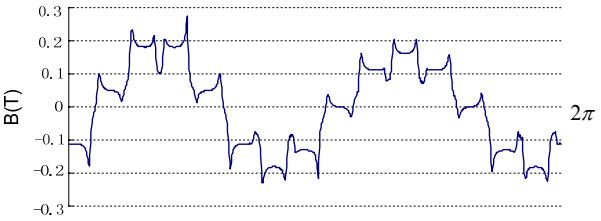

(a) Flux density distribution

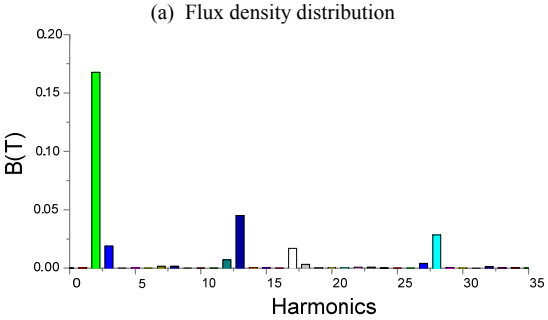

(b) Harmonic contents

Figure.13 Flux densities and its harmonic contents (coil span = 2)

At $\omega t = \pi / 2$, under one-phase winding open-circuit fault conditions and after improvement, the flux density distributions of the armature reaction magnetic fields are shown in Fig.14 and Fig.15.

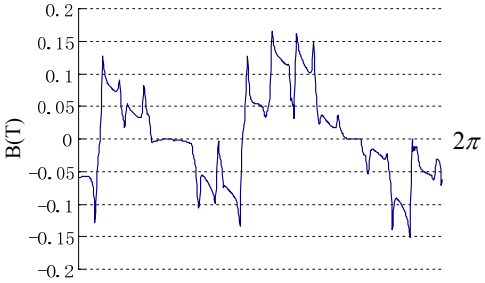

Figure.14 Flux density distribution (A-phase winding open-circuit fault)

Figure.15 Flux density distribution (after improvement)

At $\omega t = \pi / 2$, under open-circuit faults of two adjacent phase windings and two nonadjacent phase windings conditions, the flux density distributions of the armature reaction magnetic fields are shown in Fig.16 and Fig.17.

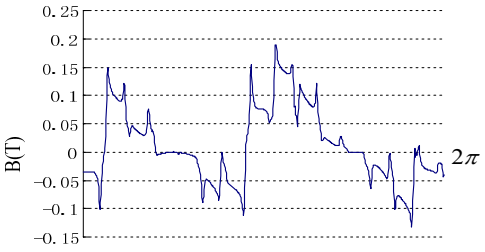

Figure.16 Flux density distribution
(open-circuit fault of A and B-phase windings)

Figure.17. Flux density distribution
(open-circuit fault of A and C-phase windings)

VI. Conclusion

The method to calculate the winding factor proposed in this paper is convenient. The armature reaction MMFs of a permanent magnet machine with 4 poles, 15 slots, and 5-phase double-layer winding are calculated. In normal working, open-circuit fault states of one-phase winding, two adjacent phase windings, and non-adjacent phase windings, the armature MMFs are calculated, and the contents of their harmonics are analyzed. In fault states, the amplitudes of the forward and reverse round rotating MMFs are calculated, discussed, and compared. The research work will contribute to understand the phenomenon of the armature winding open-faults, design fault-tolerant PMSMs, and control PMSMs in fault state.

References

[1] Ayman M. EL-Refaie, "Fractional-Slot Concentrated-Windings Synchronous Permanent Magnet Machines: Opportunities and Challenges," *IEEE Transactions on Industrial Electronics*, vol. 57, no. 1, pp. 107–121, 2011.

[2] Nicola Bianchi, Emanuele Fornasiero, "Impact of MMF Space Harmonic on Rotor Losses in Fractional-Slot Permanent- Magnet Machines," *IEEE Transactions on Energy Conversion*, vol. 24, no. 2, pp. 323–328, 2009.

[3] AymanM. ElRefaie, Thomas M.Jahns, DonaldW. Novotny, "Analysis of Surface Permanent Magnet Machines with Fractional-Slot Concentrated Windings," *IEEE Transactions on Energy Conversion*, vol. 21, no. 1, pp. 34 –43, 2006.

[4] L. J. Wu, Z. Q. Zhu, J. T. Chen, Z. P. Xia, and Geraint W. Jewell, "Optimal Split Ratio in Fractional-Slot Interior Permanent-Magnet Machines With Non-Overlapping Windings," *IEEE Transactions on Magnetics*, vol. 46, no. 5, pp. 1235–1242, 2010.

[5] Leila Parsa, Hamid A. Toliyat, Abas Goodarzi, "Five-Phase Interior Permanent-Magnet Motors with Low Torque Pulsation," *IEEE Transactions on Industrial Applications*, vol. 43, no. 1, pp. 40–46, 2007.

[6] Nicola Bianchi, Silverio Bolognani, Dai Pré, "Impact of Stator Winding of a Five-Phase Permanent-Magnet Motor on Postfault Operations," *IEEE Transactions on Industrial Applications*, vol. 55, no. 5, pp. 1978–1987, 2008.

[7] Nicola Bianchi, Silverio Bolognani, Michele Dai Pre, "Strategies for the Fault-Tolerant Current Control of a Five-Phase Permanent-Magnet Motor," *IEEE Transactions on Industrial Applications*, vol. 43, no. 4, pp. 960–970, 2007.

[8] Shah, Manoj R.,El-Refaie, Ayman M, "End effects in multiphase fractional slot concentrated-winding surface permanent magnet synchronous machines," *IEEE Transactions on Energy Conversion*, vol. 25, no. 4, pp. 1001–1009,2010.

[9] El-Refaie, Ayman M, "Rotor end losses in multiphase fractional-slot concentrated-winding permanent magnet synchronous machines," *IEEE Transactions on Industrial Applications*, vol. 47, no. 5, pp. 2066–2074, 2007.

[10] Kestelyn, Xavier1, Semail, Eric1, "A vectorial approach for generation of optimal current references for multiphase permanent-magnet synchronous machines in real time," *IEEE Transactions on Industrial Electronics,* vol.58, no.11, pp. 5057-5065, 2011.

Xuanfeng Shangguan received the B.Sc. and M.Sc. degrees in electrical power engineering in 1988 and 1991, respectively, from Henan Polytechnic University, Jiaozuo, China, and Ph.D. degree in electrical power engineering in 2006 from Xi'an Jiaotong University.

Since 2008, he has been a Professor with the Department of Electrical Engineering, Henan Polytechnic University. He is working in the Institute of Linear Electric Machines and Modern Drives. His interests include electrical machines and drives.

Jiaolong Zhang was born in China in 1977. He received her B.Sc. degree from Liaoning Shihua University in 2001, and M.Sc. degree from Henan Polytechnic University in 2010, all in Control Theory and Control Engineering. From 2001 to 2007, He served as a teacher at School of Electrical Engineering & Automation, Jiaozuo, China. From 2007 to 2010, He studied at Department of Electrical Engineering & Automation of Henan Polytechnic University. He has published 5 papers in international journals and conferences. His research interests include complex nonlinear system control and application, robust control and fuzzy control of systems with time-delay.